Performance of the Spin-Flip and Multireference Methods for Bond Breaking in Hydrocarbons: A Benchmark Study

Anna A. Golubeva,[†,‡] Alexandr V. Nemukhin,[‡] Stephen J. Klippenstein,[£] Lawrence B. Harding,[£] and Anna I. Krylov*[,†]

Department of Chemistry, University of Southern California, Los Angeles, California 90089-0482, Department of Chemistry, Moscow State University, Moscow 119899, Russian Federation, and Chemistry Division, Argonne National Laboratory, Argonne, Illinois 60439

Received: August 9, 2007; In Final Form: September 20, 2007

Benchmark results for spin-flip (SF) coupled-cluster and multireference (MR) methods for bond-breaking in hydrocarbons are presented. The nonparallelity errors (NPEs), which are defined as an absolute value of the difference between the maximum and minimum values of the errors in the potential energy along bond-breaking curves, are analyzed for (i) the entire range of nuclear distortions from equilibrium to the dissociation limit and (ii) in the intermediate range (2.5−4.5 Å), which is the most relevant for kinetics modeling. For methane, the spin-flip and MR results are compared against full configuration interaction (FCI). For the entire potential energy curves, the NPEs for the SF model with single and double substitutions (SF-CCSD) are slightly less than 3 kcal/mol. Inclusion of triple excitations reduces the NPEs to 0.32 kcal/mol. The corresponding NPEs for the MR-CI are less than 1 kcal/mol, while those of multireference perturbation theory are slightly larger (1.2 kcal/mol). The NPEs in the intermediate range are smaller for all of the methods. The largest errors of 0.35 kcal/mol are observed, surprisingly, for a spin-flip approach that includes triple excitations, while MR-CI, CASPT2, and SF-CCSD curves are very close to each other and are within 0.1−0.2 kcal/mol of FCI. For a larger basis set, the difference between MR-CI and CASPT2 is about 0.2 kcal/mol, while SF-CCSD is within 0.4 kcal/mol of MR-CI. For the C−C bond breaking in ethane, the results of the SF-CCSD are within 1 kcal/mol of MR-CI for the entire curve and within 0.4 kcal/mol in the intermediate region. The corresponding NPEs for CASPT2 are 1.8 and 0.4 kcal/mol, respectively. Including the effect of triples by energy-additivity schemes is found to be insignificant for the intermediate region. For the entire range of nuclear separations, sufficiently large basis sets are required to avoid artifacts at small internuclear separations.

1. Introduction

At equilibrium, the wave functions of well-behaved closed-shell molecules are dominated by a single electronic configuration, a Hartree−Fock determinant, and, therefore, can be described by single-reference methods. At the dissociation limit, at least two electronic configurations become equally important, for example, $(\sigma)^2$ and $(\sigma^*)^2$ for a single σ-bond breaking. Thus, to describe potential energy profiles for bond breaking, an approximate wave function should be sufficiently flexible to treat both configurations on the same footing.[1] Moreover, for quantitative accuracy, dynamical correlation should also be included. This can be achieved, for example, by employing a multiconfigurational self-consistent field (MCSCF or CASSCF) reference[2,3] within multireference configuration interaction (MRCI) or perturbation theory (MRPT) schemes.[4] Among those approaches are MR-CISD, which includes all singly and doubly excited determinants from the MSCSF reference,[5−7] and the CASPT2 method.[8,9] To correct for the lack of size-extensivity, the former is often augmented by the Davidson correction.[10]

Alternatively, single-bond breaking can be modeled by spin-flip (SF) methods that describe the target multiconfigurational wave function as spin-flipping excitations from a well-behaved high-spin triplet, for example, $|\sigma\alpha\sigma^*\alpha>$ reference.[11,12] By employing theoretical models of increasing complexity for the reference wave function, the description of the target SF states can be systematically improved.[11−18] Other single-reference methods capable of describing bond breaking include completely renormalized CC methods[19,20] and a host of CC techniques exploiting active-space ideas.[21−24] For a comprehensive recent review on bond-breaking methods, see ref 1.

For practical applications, the critical concern is accuracy versus cost. The assessment of the former requires extensive calibration[25] against benchmark data, either experimental or theoretical. Since potential energy surfaces (PESs) cannot be directly measured, the calibration against experimental data involves several modeling steps, each step introducing an error (e.g., calculation of rate constants requires dynamics, etc.). These errors may add up or cancel out, making it difficult to establish reliable error bars for an electronic structure method. Moreover, experimental quantities are seldom equally sensitive to the entire PES. Thus, only calibration against reliable theoretical PESs allows unambiguous characterization of the errors introduced by approximations in solving the Schrödinger equation. Moreover, it also allows one to separate errors due to finite one-electron basis sets versus errors introduced by incomplete correlation treatments.

The ultimate reference for assessing the accuracy of a correlation treatment is, of course, full CI (FCI) data. Unfortunately, these are available only for relatively small systems

[†] University of Southern California.
[‡] Moscow State University.
[£] Argonne National Laboratory.

10.1021/jp0764079 CCC: $37.00
Published on Web 11/16/2007

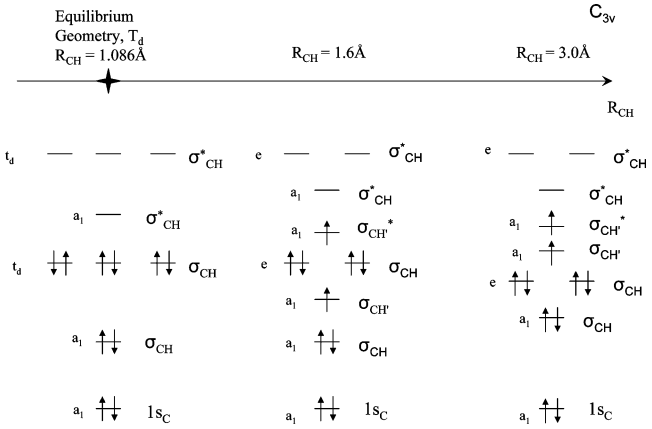

Figure 1. Changes in methane MOs along the C−H bond-breaking coordinate. The ground-state electronic configuration is shown at the equilibrium geometry. At an elongated CH bond, the electronic configuration of the triplet reference state is shown.

and moderate one-electron bases. Because of the slow convergence of correlation energy with respect to one-electron basis (due to the two-electron cusp), the errors due to an incomplete correlation treatment may increase with the basis set size, and therefore, benchmarks using large basis sets (and necessarily more approximate correlation treatments) are important. The transferability of the benchmark results to larger systems requires size-extensivity. The accuracy of methods that are not rigorously size-extensive is expected to deteriorate with molecular size.

Recent benchmark studies of Sherrill and co-workers[26,27] investigated the performance of several single and multireference methods for breaking bonds to hydrogen. Their benchmark data set included a FCI/6-31G* PES for methane. Among other methods, Abrams and Sherrill[27] characterized the performance of MR-CISD and CASPT2, including the sensitivity of the methods to the active-space choice. The choice of the latter, as well as scaling consequences, requires additional comments. The minimal active space for breaking a single bond consists of two electrons in two orbitals, σ and σ^*. The cost and scaling of the corresponding (2,2) MCSCF is similar to that of regular Hartree−Fock (HF). Consequently, CASPT2 and MR-CISD employ such a reference scale as single-reference MP2 and CISD, that is, N^5 and N^6, respectively. A more flexible and less ambiguous choice is a full-valence active space. Furthermore, an argument can be made in favor of a larger, so-called one-to-one active space, which includes all occupied valence orbitals plus a virtual active orbital (of the same symmetry) for each active occupied orbital. In the case of methane, full-valence and one-to-one active spaces are identical. The size of these spaces increases rapidly with molecular size, and such calculations quickly become unfeasible due to the factorial scaling of the underlying MCSCF calculation. Abrams and Sherrill only compared full-valence and one-to-one active spaces. They found that the corresponding MR-CISD parallels the FCI curves very well, the NPEs (nonparallelity errors) being 0.29−0.04 kcal/mol for the one-to-one active space. The CASPT2 errors were found to be larger, for example, 3.3 kcal/mol. Both methods show larger errors around equilibrium, where dynamical correlation is more important.[22] Surprisingly, CASPT2 was found to be less sensitive to the active-space choice. Unfortunately, MR-CISD is not size-extensive, and the above error bars will increase in larger molecules. CASPT2 is approximately size-extensive, and one may expect similar performance in larger systems.

In this work, we consider CASPT2 and MR-CISD using a minimal (2,2) active space. We also employ the Davidson size-extensivity correction[10] for MR-CISD (denoted as MR-CISD+Q). We analyzed the NPEs of potential energy curves for (i) the entire range of nuclear distortions from equilibrium to the dissociation limit and (ii) in the intermediate range (2.5−4.5 Å), which is the most relevant for kinetics modeling.[28,29]

All SF models are size-extensive (or, more precisely, core-extensive),[30−32] as explained in footnote 32 in ref 12. Similar to regular equation-of-motion coupled-cluster (EOM-CC) and CI methods, the accuracy of the SF models depends on the highest excitation level present in EOM and CC operators. The simplest model, SF-CIS, which includes just single excitations, only provides a qualitatively correct zero-order wave function of, approximately, MCSCF quality. The accuracy of EOM-SF-CCSD (which includes singles and doubles) for energy differences approaches 1 kcal/mol, as follows from the benchmark study on the singlet−triplet gaps in diradicals,[33] and one might expect similar performance for bond breaking. Not surprisingly, the explicit inclusion of all triple excitations[18] results in a significant improvement, for example, consistent with EOM-

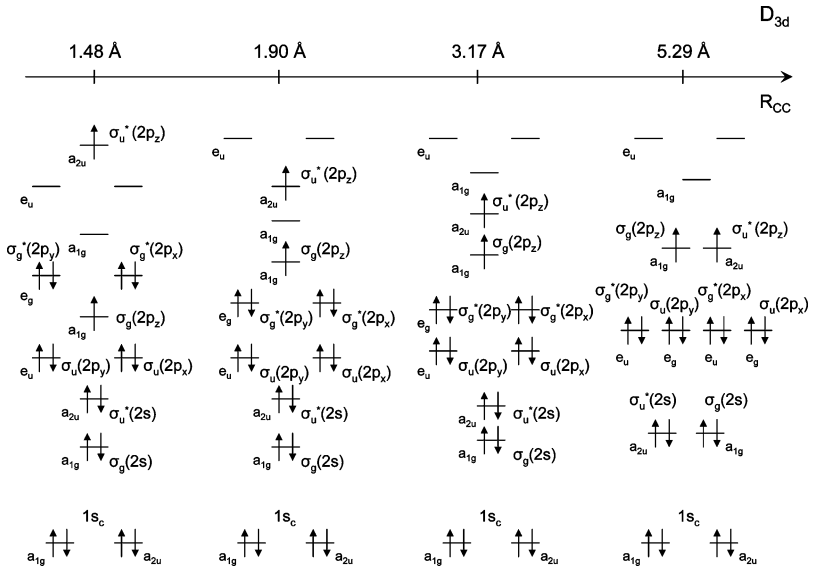

Figure 2. Molecular orbitals of ethane along the C−C bond-breaking coordinate. The electronic configuration of the triplet reference state employed in the SF calculations is shown.

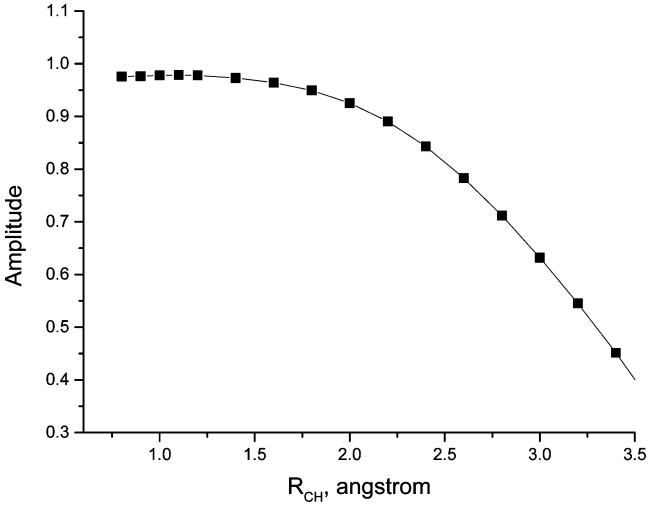

Figure 3. The weight of the $(\text{core})^2(\sigma_{CH})^6(\sigma_{CH'})^2$ configuration in the EOM-SF-CCSD wave function along the C−H′ bond-breaking coordinate (methane, 6-31G*).

TABLE 1: Total Hartree−Fock and CCSD Energies (hartrees) for the UHF and ROHF Triplet References for Methane and Ethane; $<S^2>$ Values Are Also Shown

reference	E^{HF}	E^{CCSD}	$\langle S^2 \rangle$
ROHF[a]	−39.726073	−39.907011	
UHF[a]	−39.731212	−39.906588	2.0164
UHF[b]	−78.897288	−79.280507	2.0166

[a] Methane, at tetrahedral geometry ($R_{CH} = R_{CH'} = 1.086$ Å), 6-31G* basis set. [b] Ethane, with the methyl groups frozen at planar staggered configuration and $R_{CC} = 1.58754$ Å, aug-cc-pVTZ basis set.

CC for excitation energies (EOM-EE-CC) benchmarks,[34] and one may expect sub-kcal/mol accuracy. While EOM-CCSD[11,17] calculations are affordable for moderate-size molecules (the scaling of EOM-CCSD is N^6), the explicit inclusion of triples[18] brings the scaling to N^8, making such calculations feasible only for small molecules and moderate bases. In the context of EOM-EE, several energy-additivity schemes, in which effects of triples are evaluated in small bases, were suggested. Moreover, one may account for some of the triples correction by considering only a reduced (active-space) subset of triples. We found these approaches to be useful for energy separations between electronic states in diradicals and triradicals[18,35,36] as well as excited states,[37] and in this paper, we investigate their performance in the context of bond breaking. For example, such a scheme would estimate the target EOM-EE-CCSDT large basis set energies as a sum of the CCSD energy in a large basis set and the CCSDT−CCSD difference in a small basis set

$$E^{\text{large}}_{\text{EOM-CCSDT}} \approx E^{\text{large}}_{\text{EOM-CCSD}} + (E^{\text{small}}_{\text{EOM-CCSDT}} - E^{\text{small}}_{\text{EOM-CCSD}}) \quad (1)$$

We consider two examples of bond breaking which are relevant to combustion, CH bond breaking in methane and CC bond breaking in ethane. For methane, FCI/6-31G* data allow us to assess the accuracy of both the MR and SF methods. In larger bases, and in ethane, the SF methods are compared against multireference results. The structure of the paper is as follows. The next section describes computational details. The results for methane and ethane are presented and discussed in sections 2.1 and 2.2, respectively. Our concluding remarks are given in section 3.

2. Computational Details

All multireference calculations employed a (2,2) MCSCF reference. In the MR-CISD, CASPT2, and SF calculations, the core orbitals were frozen. Internally contracted MR-CI code has been used. The MR-CISD energies were corrected by the Davidson size-extensivity correction, denoted as MR-CISD+Q. For CH_3 + H, MR-CISD+Q calculations were also done for a full-valence active space and found to yield essentially identical interaction energies.

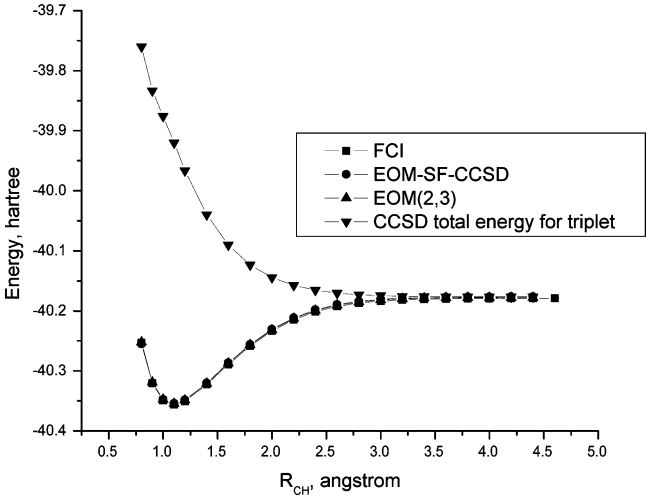

Figure 4. Total energies for the ground singlet and excited triplet states of methane along the C−H bond-breaking coordinate.

SF calculations were performed using the Q-Chem electronic structure package.[38] All MR results were obtained with MOLPRO.[39]

In both methane and ethane, the SF calculations employed the $|\sigma\alpha\sigma^*\alpha>$ triplet reference. The relevant molecular orbitals (MOs), as well as electronic configurations, are shown in Figures 1 and 2. The dominant electron configurations of the corresponding ground singlet states are

$$(\text{core})^2(\sigma_{CH})^6(\sigma_{CH'})^2(\sigma^*_{CH'})^0 - \lambda(\text{core})^2(\sigma_{CH})^6(\sigma_{CH'})^0(\sigma^*_{CH'})^2 \quad (2)$$

and

$$(\text{core})^2(\sigma_g)^2(\sigma^*_u)^2(\sigma_u)^4(\sigma^*_g)^4(\sigma_g)^2(\sigma^*_u)^0 - \lambda(\text{core})^2(\sigma_g)^2(\sigma^*_u)^2(\sigma_u)^4 (\sigma^*_g)^4(\sigma_g)^0(\sigma^*_u)^2 \quad (3)$$

where the coefficient λ depends on the bond length. Figure 3 shows the weight of the $...(\sigma_{CH'})^2$ configuration in the SF-CCSD wave function along the bond-breaking coordinate. At the equilibrium geometry, this configuration is dominant, and consequently, the coefficient λ is small. As the C−H distance increases, its weight decreases mildly and then falls rapidly to very small values between 2 and 3.5 Å. The analysis of the SF-CCSD wave function in this region shows that several other configurations become important at large $R_{CH'}$.

The EOM-SF model is not fully spin-adapted, and its performance may be effected by spin contamination of the open-shell reference. However, in the studied systems, the spin contamination of the UHF triplet reference was very small; see Table 1 for selected values. For instance, the value of $\langle S^2 \rangle_{\text{UHF}}$ for the triplet reference equals 2.0164 and 2.0166 for methane at the equilibrium ground-state geometry and ethane at the chosen geometry (described below) and with a C−C bond length of 1.58754 Å, respectively. Both molecules show no significant variation of the $\langle S^2 \rangle$ value along the dissociation curve. To assess the difference between UHF and ROHF references (which becomes significant when spin contamination is large), we considered both references in 6-31G* methane calculations. In all other calculations, UHF references were employed. We

TABLE 2: Total FCI Energies and the Errors against FCI (hartrees) for EOM-SF-CCSD, EOM-SF(2,3̃), and EOM-SF(2,3) with the 6-31G* Basis Set for Methane[a]

R_{CH}, Å	E^{FCI}	$\Delta E_{UHF}^{SF\text{-}CCSD}$	$\Delta E_{ROHF}^{SF\text{-}CCSD}$	$\Delta E_{UHF}^{SF(2,\tilde{3})}$	$\Delta E_{UHF}^{SF(2,3)}$	$\Delta E_{ROHF}^{SF(2,3)}$
0.8	−40.253342	0.001824		−0.003549	−0.001331	
0.9	−40.320513	0.000066	0.000191	−0.003848	−0.001430	−0.001452
1.0	−40.349369	−0.001776	−0.001644	−0.003949	−0.001613	−0.001606
1.1	−40.356202	−0.001958	−0.001745	−0.003567	−0.001694	−0.001680
1.2	−40.350579	−0.002084	−0.001837	−0.003318	−0.001699	−0.001677
1.4	−40.322605	−0.002424	−0.002155	−0.003061	−0.001679	−0.001648
1.6	−40.289114	−0.002643	−0.002378	−0.002899	−0.001666	−0.001638
1.8	−40.258549	−0.002775	−0.002519	−0.002714	−0.001676	−0.001651
2.0	−40.233555	−0.002850	−0.002605	−0.002547	−0.001704	−0.001674
2.2	−40.214618	−0.002881	−0.002646	−0.002457	−0.001743	−0.001717
2.4	−40.201257	−0.002881	−0.002654	−0.002422	−0.001784	−0.001756
2.6	−40.192439	−0.002864	−0.002643	−0.002419	−0.001817	−0.001787
2.8	−40.186932	−0.002840	−0.002627	−0.002427	−0.001834	−0.001800
3.0	−40.183629	−0.002814	−0.002607	−0.002439	−0.001830	−0.001792
3.2	−40.181699	−0.002791	−0.002592	−0.002450	−0.001801	−0.001755
3.4	−40.180583	−0.002765	−0.002580	−0.002457	−0.001735	−0.001678
3.6	−40.179941	−0.002735	−0.002573	−0.002463	−0.001636	−0.001566
3.8	−40.179569	−0.002692	−0.002568	−0.002463	−0.001523	−0.001446
4.0	−40.179356	−0.002642	−0.002567	−0.002461	−0.001433	−0.001353
4.2	−40.179234	−0.002596	−0.002565	−0.002452	−0.001374	−0.001293
4.4	−40.179167	−0.002566	−0.002564	−0.002439	−0.001340	−0.001258
4.6	−40.179132	−0.002550	−0.002565	−0.002549	−0.001327	−0.001241

[a] FCI energies from ref 26. Because of the ROHF convergence problems, we were not able to calculate ROHF-based values at 0.8 Å.

would like to emphasize that using ROHF references in any open-shell EOM-CC calculations yields consistently better results and is therefore strongly recommended. However, due to better convergence in the UHF SCF procedure, we employed inferior UHF references for computational convenience.

The methane potential energy curves were obtained by altering the length of a single C−H bond with all of the remaining atoms fixed. Two different geometries were employed for the CH_3 moiety. The first geometry (used in small basis calculations) is from refs 26 and 27 and can be described as a tetrahedral methane with one C−H bond being stretched from 0.8 to 4.6 Å and the three other bonds frozen at 1.086 Å. The second geometry was employed in aug-cc-pVTZ calculations. It corresponds to a planar CH_3 radical bonded to a hydrogen atom (H′) such that the C−H′ bond is perpendicular to the radical plane. This geometry better describes the structure in the intermediate region along the dissociation curve, which is most important for kinetics modeling.[28,29] The length of the C−H′ bond was varied from 1.05 to 4.23 Å.

The dissociation curves in ethane were obtained by varying the C−C bond from 1.05 to 5.29 Å, with the methyl groups frozen in a planar geometry (R_{CH} = 1.084819 Å), with an overall staggered D_{3d} configuration.

In methane, we employed the 6-31G* basis for which FCI results are available, as well as the large aug-cc-pVTZ basis. For ethane, we only considered the aug-cc-pVTZ basis. Additional calculations were performed for the 6-31G, 6-31G**, and 6-311G** bases for methane and the 6-31G* basis for ethane to investigate the performance of energy-additivity schemes.

To assess the accuracy of different SF models, we performed our calculations within the regular EOM-SF-CCSD and EOM-SF, with triple excitations included in the EOM part,[18] EOM-SF(2,3), as well as its less expensive active-space counterpart, EOM-SF(2,3̃). The latter includes only a small subset of triple excitations in which at least one electron is excited to or from σ and σ^* orbitals. Finally, the energy-additivity scheme of eq 1 was also employed.

2.1. Bond Breaking in Methane. *2.1.1. 6-31G* Results.* Figure 4 shows the potential energy curves for the ground X^1A_1 and the reference triplet states. As the two SF ground-state curves and the FCI curve appear very close on this scale, we will be showing errors against the FCI curve from now on. The NPE was computed as an absolute value of the difference between the largest and the smallest values of the error curve.

TABLE 3: Maximum and Minimum Absolute Errors and NPE (kcal/mol) against FCI for Selected Methods with the 6-31G* Basis Set for the Methane Example

	ΔE_{max}^{abs}	ΔE_{min}^{abs}	NPE
EOM-SF-CCSD	1.81	0.04	2.95
EOM-SF(2,3̃)	2.48	1.52	0.96
EOM-SF(2,3)	1.15	0.84	0.32
CCSD	6.69	1.60	5.09
CASSCF(4,4)	51.91	45.57	6.34
CASSCF(2,2)	93.08	84.40	8.69
CASPT2(4,4)	7.62	6.06	1.56
CASPT2(2,2)	13.41	12.24	1.17
MR-CISD(4,4)	0.97	0.67	0.31
MR-CISD(2,2)	4.80	4.23	0.57
MR-CISD+Q(2,2)	0.22	0.06	0.16

[a] CCSD and FCI results from ref 26. Full-valence (4,4) CASSCF, CASPT2, and MR-CISD are from ref 27.

Table 2 gives the ground-state total energy errors for methane with the 6-31G* basis for the three SF models employing UHF and ROHF references. The 6-31G* results are summarized in Table 3, where the corresponding maximum and minimum errors and the NPEs are provided. The NPEs of EOM-SF-CCSD and EOM-SF(2,3) are 2.95 and 0.32 kcal/mol, respectively. Note that the EOM-SF-CCSD error changes sign. The NPE of the active-space EOM-SF(2,3̃) is 0.96 kcal/mol. The NPE of CASPT2 is above 1 kcal/mol. The NPEs of MR-CISD and MR-CISD+Q are 0.57 and 0.16 kcal/mol, respectively. The gap between the raw MR-CISD data and the Davidson-corrected results will increase with molecular size due to the lack of size-extensivity of the former.

As can be seen from Figure 5, the results are rather insensitive to the reference choice (ROHF or UHF), which is consistent with moderate spin contamination of the UHF reference (see Table 1). Figure 6 shows the errors of the selected methods along the bond-breaking coordinate. Note that the largest values

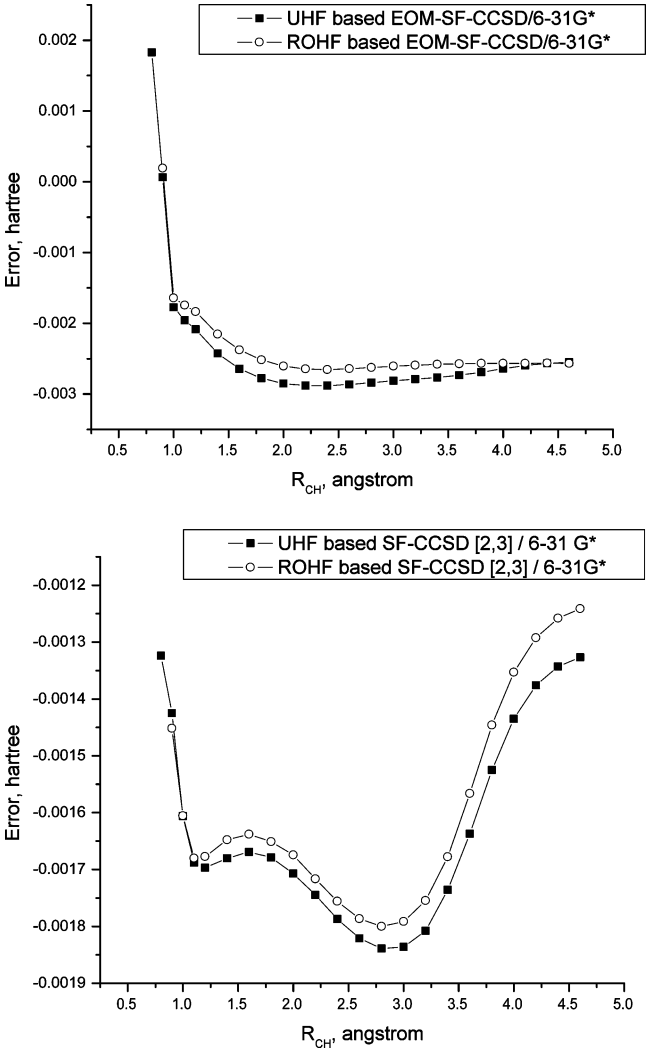

Figure 5. Methane, 6-31G* basis set. Errors of EOM-SF-CCSD (upper panel) and EOM-SF(2,3) (lower panel) against FCI. Different scales are used.

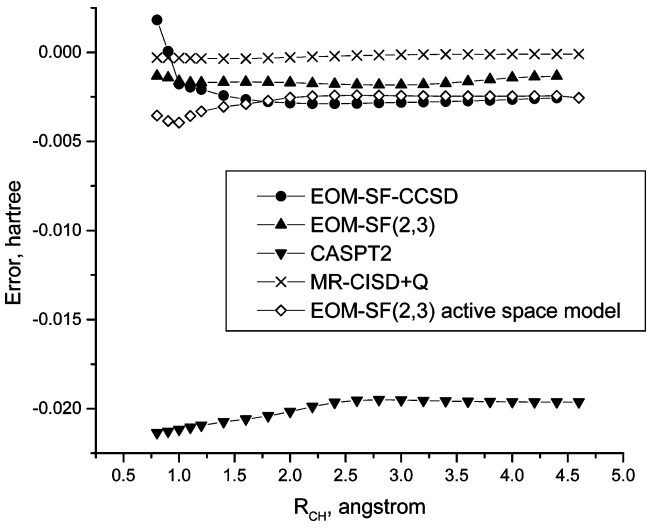

Figure 6. Errors of selected methods against FCI results for methane in the 6-31G* basis set.

and the greatest variations in the NPEs occur at short distances, that is, around the equilibrium geometry.

The errors in the intermediate region, of importance to transition-state theory-based kinetic estimates, are shown in Figure 7. Note that it is in the intermediate region, where

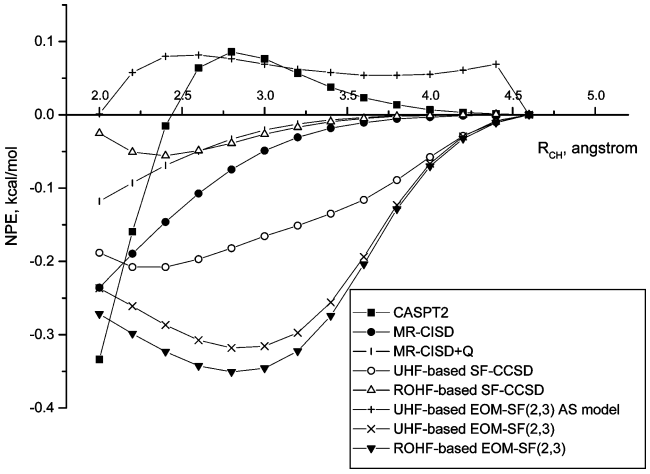

Figure 7. Methane, 6-31G*. Errors of selected methods in the intermediate region. All curves are shifted such that the energies at 4.6 Å are equal to zero.

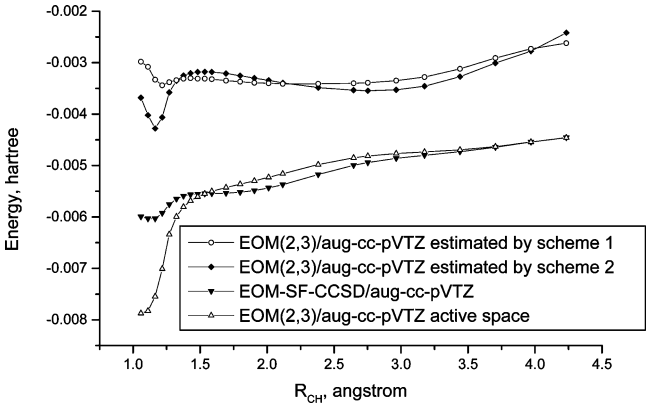

Figure 8. Errors of EOM-SF-CCSD and EOM-SF(2,3) (estimated from results for the 6-311G** basis) against MR-CISD+Q results for the aug-cc-pVTZ basis set for methane.

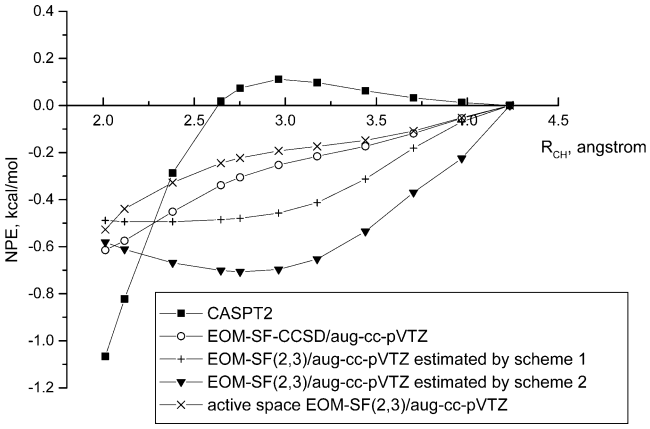

Figure 9. Methane, aug-cc-pVTZ. Errors of selected methods against MR-CISD+Q in the intermediate region. All curves are shifted such that the energies at 4.6 Å are equal to zero.

the character of the wave function undergoes rapid changes (Figure 3). Thus, only methods that faithfully reproduce this change can yield small NPEs in this region. All curves are shifted such that their values at the dissociation limit are zero. On this scale, the small differences in the PES shapes become discernible. For example, the MR-CISD+Q and ROHF-based SF-CCSD curves are very close to each other and are the most parallel to FCI, within 0.10 kcal/mol, while the NPE of UHF-based SF-CCSD is 0.15 kcal/mol. Quite surprisingly, the errors

TABLE 4: Total MR-CISD+Q Energies and the Errors against MR-CISD+Q (hartrees) for CASPT2, EOM-SF-CCSD, EOM-SF(2,3) (Estimated from 6-311G Results), and EOM-SF(2,$\tilde{3}$) with the aug-cc-pVTZ Basis Set for Methane**

R_{CH}, Å	$E^{MR\text{-}CISD+Q}$	ΔE^{CASPT2}	$\Delta E_{UHF}^{SF\text{-}CCSD}$	$\Delta E_{UHF}^{SF(2,3)_a}$	$\Delta E_{UHF}^{SF(2,3)_b}$	$\Delta E_{UHF}^{SF(2,\tilde{3})}$
1.05836	−40.402437	−0.023392	−0.005994	−0.002979	−0.003680	−0.007873
1.11128	−40.405344	−0.023333	−0.006034	−0.003080	−0.004021	−0.007826
1.16420	−40.405255	−0.023274	−0.006033	−0.003326	−0.004278	−0.007545
1.21711	−40.402971	−0.023213	−0.005926	−0.003436	−0.004064	−0.007009
1.27003	−40.399097	−0.023149	−0.005759	−0.003384	−0.003576	−0.006338
1.32295	−40.394098	−0.023081	−0.005651	−0.003336	−0.003352	−0.005994
1.37587	−40.388325	−0.023007	−0.005593	−0.003311	−0.003250	−0.005804
1.42879	−40.382049	−0.022924	−0.005566	−0.003303	−0.003203	−0.005687
1.48170	−40.375476	−0.022832	−0.005553	−0.003305	−0.003182	−0.005607
1.53462	−40.368762	−0.022728	−0.005547	−0.003312	−0.003178	−0.005548
1.58754	−40.362026	−0.022612	−0.005544	−0.003322	−0.003181	−0.005501
1.69338	−40.348827	−0.022343	−0.005538	−0.003347	−0.003210	−0.005427
1.79921	−40.336359	−0.022027	−0.005520	−0.003371	−0.003252	−0.005362
1.90505	−40.324886	−0.021669	−0.005487	−0.003390	−0.003300	−0.005299
2.01088	−40.314546	−0.021285	−0.005435	−0.003402	−0.003344	−0.005299
2.11672	−40.305401	−0.020896	−0.005372	−0.003411	−0.003392	−0.005159
2.38131	−40.287696	−0.020043	−0.005175	−0.003411	−0.003484	−0.004981
2.64590	−40.276476	−0.019556	−0.004996	−0.003397	−0.003536	−0.004849
2.75174	−40.273422	−0.019468	−0.004942	−0.003388	−0.003545	−0.004814
2.96341	−40.269109	−0.019408	−0.004859	−0.003352	−0.003528	−0.004766
3.17508	−40.266499	−0.019430	−0.004800	−0.003282	−0.003458	−0.004736
3.43967	−40.264682	−0.019486	−0.004732	−0.003122	−0.003271	−0.004695
3.70426	−40.263755	−0.019534	−0.004645	−0.002912	−0.003007	−0.004632
3.96885	−40.263285	−0.019566	−0.004543	−0.002734	−0.002776	−0.004542
4.23344	−40.263045	−0.019586	−0.004456	−0.002624	−0.002418	−0.004459

[a] Estimated from results for the 6-311G** basis, eq 4. [b] Estimated from results for the 6-311G** basis, eq 5.

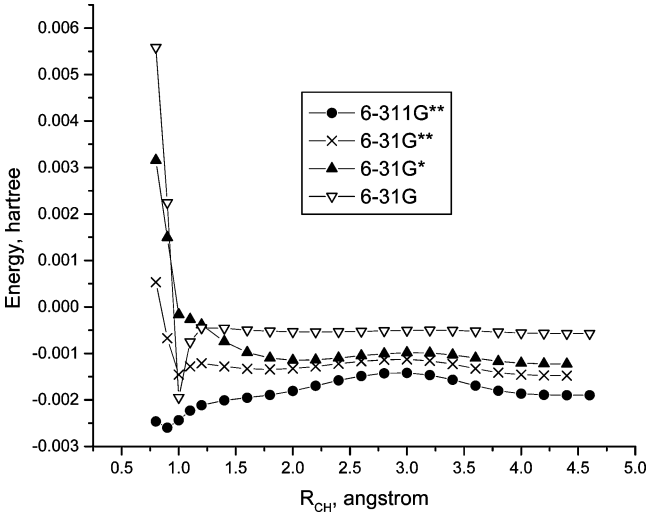

Figure 10. Difference between the EOM-SF(2,3) and EOM-SF-CCSD methane total energies for different bases.

of SF-CC(2,3) are somewhat larger—about 0.35 kcal/mol—and more irregular. The NPE of CASPT2 is also quite small, being about 0.1 kcal/mol.

2.1.2. Aug-cc-pVTZ Results. In this section, we compare the results of SF and CASPT2 against Davidson-corrected MR-CISD(2,2), along the PES scan that leads to planar CH_3 (see Section 2). On the basis of the results of the previous section, we expect the errors of MR-CISD+Q to be of a sub-kcal/mol range, for example, 0.1 to 0.2 kcal/mol.

The errors are presented in Table 4 and Figures 8 and 9. Similar to the small basis results, the SF errors are largest around the equilibrium, while the long-range part of the curve faithfully parallels MR-CISD+Q. In the intermediate region, the NPEs of SF-CCSD and CASPT2 are much smaller than those for the entire curve.

Using this example, we investigated the performance of several energy-additivity schemes described in section 2. As

TABLE 5: Maximum and Minimum Absolute Errors and NPE (kcal/mol) against MR-CISD+Q for Selected Methods with the aug-cc-pVTZ Basis Set for Methane

	ΔE_{max}^{abs}	ΔE_{min}^{abs}	NPE
EOM-SF-CCSD	3.79	2.80	0.99
EOM-SF(2,3)[a]	2.16	2.65	0.51
EOM-SF(2,3)[b]	2.68	1.51	1.17
EOM-SF(2,$\tilde{3}$)	4.94	2.80	2.14
CASPT2	14.68	12.18	2.50

[a] Estimated from results for the 6-311G** basis, eq 4. [b] Estimated from results for the 6-311G** basis, eq 5.

one can see from Figure 10, a sufficiently large basis set is required to reliably evaluate the effect of triple excitations. Disappointingly, for bases smaller than 6-311G**, large irregular errors around equilibrium are spoiling the NPEs. Using the 6-311G** basis, we also compared energy-additivity schemes based on full and active-space triples, eqs 4 and 5 , respectively

$$E_{EOM(2,3)}^{aug\text{-}cc\text{-}pVTZ} = E_{EOM-CCSD}^{aug\text{-}cc\text{-}pVTZ} + (E_{EOM(2,3)}^{6\text{-}311G^{**}} - E_{EOM\text{-}CCSD}^{6\text{-}311G^{**}}) \quad (4)$$

$$E_{EOM(2,3)}^{aug\text{-}cc\text{-}pVTZ} = E_{EOM(2,\tilde{3})}^{aug\text{-}cc\text{-}pVTZ} + (E_{EOM(2,3)}^{6\text{-}311G^{**}} - E_{EOM(2,\tilde{3})}^{6\text{-}311G^{**}}) \quad (5)$$

The results for the entire dissociation curve for the aug-cc-pVTZ basis are summarized in Figure 8 and Tables 4 and 5. These results indicate that eq 4 gives better results than the active-space-based eq 5. For example, the NPE relative to the MR-CISD+Q curve is 0.51 kcal/mol for eq 4 compared with 1.17 kcal/mol for eq 5 . Also, note that the EOM-SF-CCSD curve is within 1 kcal/mol of the MR-CISD+Q curve. The inclusion of the active-space triples does not appear to improve the results—the NPE actually increases to 2.14 kcal/mol. We attribute this to the spin contamination of EOM-SF states, which makes the results more sensitive to the orbital choice for active-space calculations.

For the CASPT2 curve, the NPE is 2.5 kcal/mol when considering the entire curve. However, as illustrated in Figure 9, the NPE decreases greatly when focusing on the intermediate

TABLE 6: Ethane, aug-cc-pVTZ; Total MR-CISD+Q Energies and Energy Differences (in hartrees) for the Selected Methods

R_{CC}, Å	$E^{MR\text{-}CISD+Q}$	ΔE^{CASSCF}	ΔE^{CASPT2}	$\Delta E^{MR\text{-}CISD}$
1.05836	−79.104823	−0.425190	−0.033202	−0.042608
1.16420	−79.301698	−0.421346	−0.034300	−0.042396
1.27003	−79.424633	−0.417812	−0.035020	−0.042263
1.37587	−79.500304	−0.414736	−0.035495	−0.042158
1.48170	−79.545648	−0.412034	−0.035839	−0.042099
1.58754	−79.571362	−0.409463	−0.036033	−0.042025
1.69338	−79.584366	−0.406861	−0.036067	−0.041908
1.79921	−79.589192	−0.404197	−0.035992	−0.041746
1.90505	−79.588831	−0.401506	−0.035850	−0.041541
2.01088	−79.585276	−0.398834	−0.035668	−0.041297
2.11672	−79.579882	−0.396230	−0.035460	−0.041022
2.22256	−79.573578	−0.393736	−0.035238	−0.040725
2.32839	−79.566996	−0.391388	−0.035016	−0.040417
2.43423	−79.560560	−0.389213	−0.034808	−0.040109
2.54006	−79.554535	−0.387230	−0.034624	−0.039810
2.64590	−79.549077	−0.385448	−0.034476	−0.039527
2.75174	−79.544258	−0.383872	−0.034369	−0.039265
2.96341	−79.536559	−0.381311	−0.034277	−0.038816
3.17508	−79.531179	−0.379451	−0.034314	−0.038472
3.43967	−79.526938	−0.377897	−0.034448	−0.038169
3.70426	−79.524529	−0.376939	−0.034596	−0.037974
3.96885	−79.523199	−0.376356	−0.034717	−0.037852
4.23344	−79.522473	−0.376000	−0.034804	−0.037775
4.76262	−79.521868	−0.375640	−0.034904	−0.037696
5.29180	−79.521692	−0.375492	−0.034947	−0.037663

TABLE 7: Ethane, aug-cc-pVTZ; The Energy Differences against MR-CISD+Q (hartrees) for EOM-SF-CCSD, EOM-SF(2,3) (Estimated from the 6-31G* Results)

R_{CC}, Å	$E^{SF(2,3)}_{6\text{-}31G^*} - E^{SF\text{-}CCSD}_{6\text{-}31G^*}$	$\Delta E^{SF(2,3)}$	$\Delta E^{SF\text{-}CCSD}$
1.05836	−0.001885		
1.16420	−0.005446	0.000015	−0.005431
1.27003	0.007011	−0.013902	−0.006891
1.37587	0.001681	−0.008621	−0.006940
1.48170	−0.000814	−0.006203	−0.007017
1.58754	−0.002023	−0.005125	−0.007148
1.69338	−0.002587	−0.004440	−0.007027
1.79921	−0.002824	−0.003974	−0.006798
1.90505	−0.002910	−0.003725	−0.006635
2.01088	−0.002917	−0.003560	−0.006477
2.11672	−0.002893	−0.003441	−0.006334
2.22256	−0.002845	−0.003365	−0.006210
2.32839	−0.002779	−0.003321	−0.006100
2.43423	−0.002700	−0.003307	−0.006007
2.54006	−0.002612	−0.003311	−0.005923
2.64590	−0.002517	−0.003339	−0.005856
2.75174	−0.002419	−0.003381	−0.005800
2.96341	−0.002239	−0.003475	−0.005714
3.17508	−0.002080	−0.003578	−0.005658
3.43967	−0.001939	−0.003676	−0.005615
3.70426	−0.001852	−0.003741	−0.005593
3.96885	−0.001801	−0.003779	−0.005580
4.23344	−0.001774	−0.003800	−0.005574
4.76262	−0.001755	−0.003813	−0.005568
5.29180	−0.001751	−0.003816	−0.005567

region of importance to kinetics. Indeed, in the region from 2.5 to 4.5 Å, the CASPT2 NPE of 0.2 kcal/mol or less is lower than the EOM-SF-CCSD NPE of 0.4 kcal/mol or less.

2.2. Bond Breaking in Ethane, aug-cc-pVTZ Basis. Table 6 contains total MR-CISD+Q energies used as the benchmark for all other methods, as well as the corresponding energy differences for CASSCF, CASPT2, and non-Davidson-corrected MR-CISD. The energy differences for the SF methods are given in Table 7. Figures 11 and 12 summarize these results graphically. Table 8 presents the maximum and minimum absolute errors, as well as NPEs. Consistent with the methane results, energy estimates from results for the 6-31G* basis give

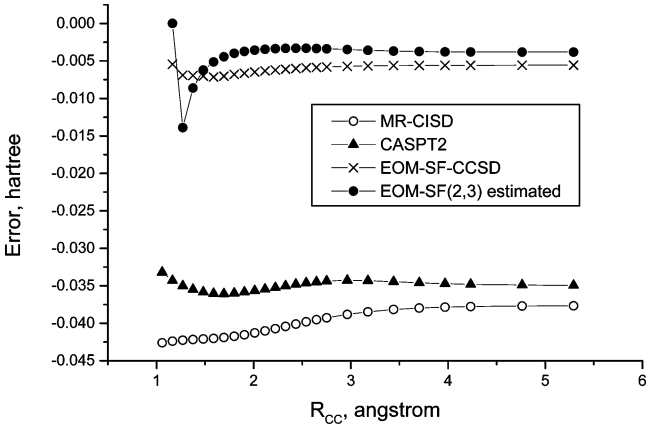

Figure 11. Errors of EOM-SF-CCSD and EOM-SF(2,3) (estimated from results for the 6-31G* basis) against MR-CISD+Q results for the aug-cc-pVTZ basis set for ethane.

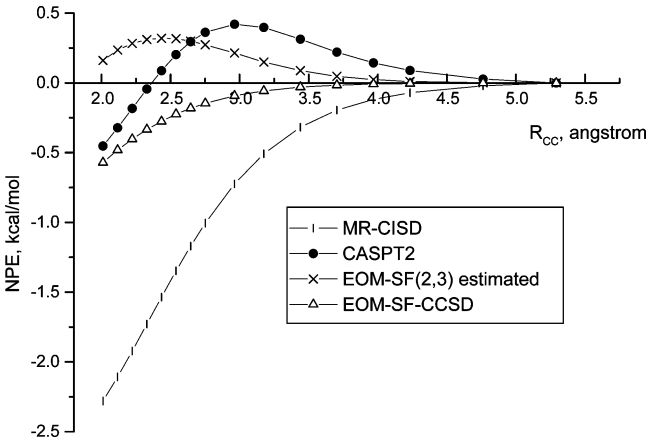

Figure 12. Ethane, aug-cc-pVTZ. Errors of selected methods against MR-CISD+Q for the region relevant to kinetics modeling. All curves are shifted such that the energies at 5.2918 Å are equal to zero.

TABLE 8: Maximum and Minimum Absolute Errors and NPE (kcal/mol) against MR-CISD+Q for Selected Methods with the aug-cc-pVTZ Basis Set for Ethane

	ΔE^{abs}_{max}	ΔE^{abs}_{min}	NPE
MR-CISD	26.74	23.63	3.10
CASPT2	22.63	20.83	1.80
EOM-SF-CCSD	4.49	3.41	1.08
EOM-SF(2,3)	8.72	0.01	8.73

a large NPE (8.73 kcal/mol) due to irregular behavior around the equilibrium. Overall, the EOM-SF-CCSD curve is in excellent agreement with the MR-CISD+Q curve, the NPE being 1.08 kcal/mol, while the CASPT2 error is 1.8 kcal/mol. Note that the Davidson correction accounts for about 3 kcal/mol of the NPEs, considerably more than that in the small methane example. In the intermediate region, the CASPT2, SF-CCSD, and SF-CC(2,3) (obtained using the energy-additivity scheme) results are within 0.4, 0.2, and 0.3 kcal/mol of the MR-CISD+Q results, respectively. Thus, CASPT2 and SF give adequate results for kinetics modeling.

3. Conclusions

Our benchmark results demonstrated that the EOM-SF-CCSD method performs very well for both C−H and C−C bond-breaking, as compared to FCI and MR-CISD+Q. Overall, the NPEs are very small at the intermediate and larger internuclear separations, and most of the total NPE originates from larger errors around the equilibrium.

For the PES scans relevant to kinetics (planar CH_3, bond lengths 2.5−4.5 Å), the EOM-SF-CCSD and CASPT2 provide results of similar accuracy, both being within about 0.5 kcal/mol. The inclusion of triples brings the errors for the entire curves below 1 kcal/mol; however, in the intermediate region the triples correction resulted in slightly greater errors. Energy-additivity schemes can be useful; however, relatively large basis sets need to be used to avoid irregular behavior near equilibrium. The Davidson correction is essential for obtaining reliable MR-CISD curves, especially when a minimal active space is employed.

Acknowledgment. This work was supported by the U.S. Department of Energy, Office of Basic Energy Sciences, Division of Chemical Sciences, Geoscience and Biosciences. The work at USC was supported under Contract Number DE-FG02-05ER15685, while that at Argonne was supported under Contract Number DE-AC02-06CH11357. We also acknowledge the use of the resources of the Center for Computational Studies of Electronic Structure and Spectroscopy of Open-Shell and Electronically Excited Species (iopenshell.usc.edu) supported by the National Science Foundation through the CRIF:CRF CHE-0625419+0624602+0625237 grant.

References and Notes

(1) Sherrill, C. D. *Annu. Rep. Comput. Chem.* **2005**, *1*, 45.
(2) Roos, B. O.; Taylor, P. R.; Siegbahn, P. E. M. *Chem. Phys.* **1980**, *48*, 157.
(3) Ruedenberg, K.; Schmidt, M. W.; Gilbert, M. M.; Elbert, S. T. *Chem. Phys.* **1982**, *71*, 41.
(4) Hirao, K., Ed. *Recent Advances in Multi-reference Methods*; World Scientific: River Edge, NJ, 1999.
(5) Bruna, P. J.; Peyerimhoff, S. D. In *Ab Initio Methods in Quantum Chemistry, I*; John Wiley & Sons: New York, 1987; pp 1−98.
(6) Werner, H. J.; Knowles, P. J. *J. Chem. Phys.* **1988**, *89*, 5803.
(7) Knowles, P. J.; Werner, H. J. *Chem. Phys. Lett.* **1988**, *145*, 514.
(8) Andersson, K.; Malmqvist, P.-Å.; Roos, B. O.; Sadlej, A. J.; Wolinski, K. *J. Phys. Chem.* **1990**, *94*, 5483.
(9) Werner, H. *Mol. Phys.* **1996**, *89*, 645.
(10) Langhoff, S. R.; Davidson, E. R. *Int. J. Quantum Chem.* **1974**, *8*, 61.
(11) Krylov, A. I. *Chem. Phys. Lett.* **2001**, *338*, 375.
(12) Krylov, A. I. *Acc. Chem. Res.* **2006**, *39*, 83.
(13) Krylov, A. I. *Chem. Phys. Lett.* **2001**, *350*, 522.
(14) Krylov, A. I.; Sherrill, C. D. *J. Chem. Phys.* **2002**, *116*, 3194.
(15) Shao, Y.; Head-Gordon, M.; Krylov, A. I. *J. Chem. Phys.* **2003**, *118*, 4807.
(16) Sears, J. S.; Sherrill, C. D.; Krylov, A. I. *J. Chem. Phys.* **2003**, *118*, 9084.
(17) Levchenko, S. V.; Krylov, A. I. *J. Chem. Phys.* **2004**, *120*, 175.
(18) Slipchenko, L. V.; Krylov, A. I. *J. Chem. Phys.* **2005**, *123*, 84107.
(19) Piecuch, P.; Włoch, M. J. *Chem. Phys.* **2005**, *123*, 224105.
(20) Piecuch, P.; Kowalski, K.; Pimienta, I. S. O.; Mcguire, M. J. *Int. Rev. Phys. Chem.* **2002**, *21*, 527.
(21) Piecuch, P.; Kucharski, S. A.; Bartlett, R. J. *J. Chem. Phys.* **1999**, *110*, 6103.
(22) Krylov, A. I.; Sherrill, C. D.; Byrd, E. F. C.; Head-Gordon, M. *J. Chem. Phys.* **1998**, *109*, 10669.
(23) Gwaltney, S. R.; Sherrill, C. D.; Head-Gordon, M.; Krylov, A. I. *J. Chem. Phys.* **2000**, *113*, 3548.
(24) Stolarczyk, L. Z. *Chem. Phys. Lett.* **1994**, *217*, 1.
(25) Helgaker, T.; Jørgensen, P.; Olsen, J. *Molecular Electronic Structure Theory*; Wiley & Sons: New York, 2000.
(26) Dutta, A.; Sherrill, C. D. *J. Chem. Phys.* **2003**, *118*, 1610.
(27) Abrams, M. L.; Sherrill, C. D. *J. Phys. Chem. A* **2003**, *107*, 5611.
(28) Harding, L. B.; Georgievskii, Y.; Klippenstein, S. J. *J. Phys. Chem. A* **2005**, *109*, 4646.
(29) Klippenstein, S. J.; Georgievskii, Y.; Harding, L. B. *Phys. Chem. Chem. Phys.* **2006**, *8*, 1133.
(30) Meissner, L.; Bartlett, R. J. *J. Chem. Phys.* **1991**, *94*, 6670.
(31) Stanton, J. F. *J. Chem. Phys.* **1994**, *101*, 8928.
(32) Nooijen, M.; Shamasundar, K. R.; Mukherjee, D. *Mol. Phys.* **2005**, *103*, 2277.
(33) Slipchenko, L. V.; Krylov, A. I. *J. Chem. Phys.* **2002**, *117*, 4694.
(34) Larsen, H.; Hald, K.; Olsen, J.; Jørgensen, P. *J. Chem. Phys.* **2001**, *115*, 3015.
(35) Slipchenko, L. V.; Krylov, A. I. *J. Phys. Chem. A* **2006**, *110*, 291.
(36) Koziol, L.; Winkler, M.; Houk, K. N.; Venkataramani, S.; Sander, W.; Krylov, A. I. *J. Phys. Chem. A* **2007**, *111*, 5071.
(37) Kowalczyk, T.; Krylov, A. I. *J. Phys. Chem. A* **2007**, *111*, 8271.
(38) Shao, Y.; Molnar, L. F.; Jung, Y.; Kussmann, J.; Ochsenfeld, C.; Brown, S.; Gilbert, A. T. B.; Slipchenko, L. V.; Levchenko, S. V.; O'Neil, D. P.; Distasio, R. A., Jr.; Lochan, R. C.; Wang, T.; Beran, G. J. O.; Besley, N. A.; Herbert, J. M.; Lin, C. Y.; Van Voorhis, T.; Chien, S. H.; Sodt, A.; Steele, R. P.; Rassolov, V. A.; Maslen, P.; Korambath, P. P.; Adamson, R. D.; Austin, B.; Baker, J.; Bird, E. F. C.; Daschel, H.; Doerksen, R. J.; Drew, A.; Dunietz, B. D.; Dutoi, A. D.; Furlani, T. R.; Gwaltney, S. R.; Heyden, A.; Hirata, S.; Hsu, C.-P.; Kedziora, G. S.; Khalliulin, R. Z.; Klunziger, P.; Lee, A. M.; Liang, W. Z.; Lotan, I.; Nair, N.; Peters, B.; Proynov, E. I.; Pieniazek, P. A.; Rhee, Y. M.; Ritchie, J.; Rosta, E.; Sherrill, C. D.; Simmonett, A. C.; Subotnik, J. E.; Woodcock, H. L., III; Zhang, W.; Bell, A. T.; Chakraborty, A. K.; Chipman, D. M.; Keil, F. J.; Warshel, A.; Herhe, W. J.; Schaefer, H. F., III; Kong, J.; Krylov, A. I.; Gill, P. M. W.; Head-Gordon, M. *Phys. Chem. Chem. Phys.* **2006**, *8*, 3172.
(39) Molpro, version 2006.1, a package of ab initio programs. Werner, H.-J.; Knowles, P. J.; Lindh, R.; Manby, F. R.; Schütz, M.; Celani, P.; Korona, T.; Rauhut, G.; Amos, R. D.; Bernhardsson, A.; Berning, A.; Cooper, D. L.; Deegan, M. J. O.; Dobbyn, A. J.; Eckert, F.; Hampel, C.; Hetzer, G.; Lloyd, A. W.; McNicholas, S. J.; Meyer, W.; Mura, M. E.; Nicklass, A.; Palmieri, P.; Pitzer, R.; Schumann, U.; Stoll, H.; Stone, A. J.; Tarroni, R.; Thorsteinsson, T. 2007; see http://www.molpro.net.